Immobilised anatase on clay mineral particles as a photocatalyst for herbicides degradation

Blain Paul, Wayde N. Martens, Ray L. Frost[•]

Discipline of Chemistry, Queensland University of Technology, Brisbane, Queensland 4001, Australia,

Abstract

Materials consisting of anatase linked to Laponite particles were synthesized by the reaction of $TiOSO_4$ with Laponite, and were used for the degradation of pesticides. All these materials were characterized by XRD, FTIR, Raman, TEM, specific surface area and porosity determinations. Based on the amount of photoactive phase per unit mass of the clay mineral, not based on the total weight of the catalysts, these porous catalysts were displaying a high degradation rate than commercial P25. The TiO_2 immobilized clay mineral catalysts can sediment in few minutes and could be readily separated out from a slurry system after the photocatalytic reaction. Settling properties of these catalysts are enormously high in aqueous media in contrast to P25.

Keywords: Clay mineral particles, anatase, adsorption, water purification, herbicides, TEM

[•] Author to whom correspondence should be addressed (r.frost@qut.edu.au)

1. Introduction

Photocatalytic degradation has been regarded as an effective and inexpensive tool for the removal of organic and inorganic pollutants from water. Many investigations have utilised an aqueous suspension of anatase (TiO_2) in various physicochemical forms, to degrade pollutants by UV illumination. The powder form of the most common commercially available photocatalyst, P25, shows significant photocatalytic activity, however due to its nanometer size, its use requires an additional and somewhat difficult operation to separate it out from the solution (Prieto-Mahaney et al., 2009). The use of binders is a method that can be used to solve problems with separation from the solution. Extensive investigations have been reported for the immobilisation of TiO_2 on a photo-chemically stable substrate (Yang and Li, 1995; Beydoun et al., 2000; Long and Yang, 2000; Zhu et al., 2002; Palmisano et al., 2007; Kuwahara et al., 2008; Yang et al., 2009). Cordierite monolith, stainless steel plates and beta-SiC foamare have been used as supports for titania fine powder (Rodriguez et al., 2009). Studies have even showed laminated silica or alumina gels with TiO_2 (Rodriguez et al., 2009). The degradation of the relatively stable molecule alachlor, has been examined by using TiO_2 film laminated on a glass tube (Ryu et al., 2003). The fabrication of TiO_2 onto the surface of a porous structure has also attracted enormous interest due to its increased surface area and hence increased oxidation potential of the catalyst (Yamashita et al., 2001; Yamashita and Anpo, 2003; Mori et al., 2007; Palmisano et al., 2007; Yamashita and Mori, 2007). The most common substrates available for use are clays, zeolites and silica based materials, due to their large surface area and chemical stability (Sterte, 1986; Liu et al., 1992; Takeda et al., 1997; Chen et al., 1999; Yang et al., 2009). For example, the preparation of TiO_2 cross-linked montmorillonite has demonstrated the usefulness of metal oxide pillars on a clay substrate to increase photocatalytic reactions (Sterte, 1986). Using a related method, another study offers the preparations of anatase crystals immobilised on silicate layers (Yang et al. 2009).

A recent study has shown the effect of ferric ions on the degradation of herbicide alachlor (Kim et al., 2005). Another herbicide, investigated for its semiconductor-mediated photocatalysed degradation, is chlorotoluron (Haque et al., 2006). When the aqueous suspension of imazaquin and titanium dioxide catalyst is exposed to UV light the herbicide is completely mineralized

(Garcia and Takashima, 2003). Effect of different TiO_2 and UV sources on the photocatalytic degradation of alachlor has been investigated (Wong and Chu, 2003). The hydrogen peroxide-assisted photocatalytic degradation of alachlor in combination with TiO_2 has been found to be an effective strategy for its removal (Wong and Chu, 2003). The mechanism of alachlor removal in a titania mediated photocatalytic process has been suggested recently (Chu and Wong, 2004).

Different titania fabrication methods can also enhance the photocatalytic activity as well as easing the separation of the catalyst from solution. Most common substrates available to use are zeolites and silica based materials due to their large surface area and chemical stability (Liu et al., 1992; Takeda et al., 1997; Chen et al., 1999). The present study represents an ongoing effort to immobilise TiO_2 on Laponite clay mineral interlayers and compare the photocatalytic degradation of ionic and non-ionic herbicides to P25, which is one of the best commercially available photocatalyst (Prieto-Mahaney et al., 2009).

2. Experimental Section

2.1. Materials

A synthetic layered clay mineral was obtained from Fernz Specialty Chemicals, Australia. It is a 2:1 layered hydrous magnesium lithium silicate consisting of two tetrahedral silica sheets sandwiching a central octahedral magnesia sheet, with the formula reported as $Na_{0.35}[Mg_{2.75}Li_{0.15}]Si_4O_{10}(OH)_2{\cdot}nH_2O$ (Rodionova et al., 1978). Laponite has a BET specific surface area of 367 m^2/g and a cation exchange capacity of 55 meq per 100 g of clay mineral. $TiOSO_4.xH_2O$ (98%) and hydrochloric acid (36%) were obtained from Fluka and were used without further purification. Tetraisopropoxytitanium (IV) ($Ti[O\text{-}CH(CH_3)_2]_4$, TPT) was purchased from Aldrich. The water used in all the experiments was purified with a milli-Q-plus system. Herbicides used in the experiments were HPLC grade and purchased from Aldrich. The TiO_2 source used for the preparation of clay mineral particles was commercial grade TiO_2 powder (P25, Degussa AG, Germany).

2.2. Sample preparation

The synthesis procedure of modified Laponite is based on previously reported work (Yang et al., 2009). An aqueous dispersion was prepared by dispersing 4.0 g of Laponite into 200 mL water, and stirred until the dispersion become homogeneous. An initial aqueous solution of $TiOSO_4$ was prepared by dissolving 128 g of $TiOSO_4.xH_2O$ into 1 L of deionised water. The required amount of the $TiOSO_4$ solution was introduced into clay mineral dispersion and the reaction mixture was agitated for at least 3 h. The mixture was transferred to an autoclave and hydrothermally treated for 24 h under autogeneous water pressure at 100, 150, 200 ^oC, respectively. The catalysts with different ratios of titanium to clay mineral were prepared using different quantities (25, 50 and 75 mL) of the stock $TiOSO_4$ solutions. The products were then separated by filtration, washed thoroughly with distilled water and dried in air. The samples were then grounded to a fine power and calcined at 500 ^oC for 20 h at a rate of 2 $^oC\ min^{-1}$. For the purpose of comparison five different photocatalysts were prepared with different hydrothermal temperatures and ratios. In sample name, the numbers in the bracket indicates the Ti/clay mineral ratio (mmol of Ti / g of clay mineral) and the numbers at the end indicating the hydrothermal temperature.

2.3. Characterisation

The infrared spectra of the samples were recorded with a diamond attenuated total reflectance (ATR) NEXUS 870 Fourier transform spectrometer (Thermo Nicolet Corp.), equipped with a mercury cadmium telluride detector. Each spectrum was obtained by averaging 64 interferograms with resolution of 4 cm^{-1}. Surface analysis based upon the N_2 adsorption/desorption technique was conducted on a micrometrics Tristar 3000 automated gas adsorption analyzer after sample pretreatment at 110 ^oC for 12 h under a flow of N_2. XRD patterns were recorded using Cu Kα radiation (λ = 1.5418 Å) on a Philips PANalytical X' pert PRO diffractometer operation at 40 kV and 40 mA with 0.25^o divergence slit, 0.5^o antiscatter slit, between 5 and 90^o (2θ). The TEM images of samples were obtained with a Philips CM 200 transmission electron microscope operating at 200kV. All Samples were recorded on a Cary 100 spectrometer with a scan band of 200 to 900 nm. Raman spectra were collected by a Spectra-Physics spectrometer (model 127) with a He-Ne laser (633 nm) at a resolution of 2 cm^{-1} in the

range between 100 and 1600 cm^{-1}. Repeated acquisitions using the highest magnification were accumulated to improve the signal-to-noise ratio in the spectra. Spectra were calibrated using the 520.5 cm^{-1} line of a silicon wafer.

2.4. Photocatalytic activity

The illumination of the photocatalysts was carried out by using a UV light source which consisted of six tubular 20 W Hg lamps (NEC, FL20BL T8), which emit a peak wavelength of c.a. 365 nm. A catalyst loading of 50 mg per 50 mL of solution was used. Due to the different solubility of pollutants, the initial concentrations of bromacil and alachlor were 10 ppm, whereas when chlorotoluron, sulfosulfuron, and imazaquin, were pollutants, the initial concentration was 5 ppm. The catalyst powder and herbicide solution were kept in Pyrex glass vessels for 30 min. of mixing in the dark to achieve a complete adsorption prior to irradiation. These reactors were placed on a magnetic stirring plate at a fixed distance of 25 cm from the lamb and the liquid surface of the reaction system. This UV light source was attached vertically to the internal top of a wood box (100 cm × 35 cm × 35 cm). One fan was positioned in order to minimize the heat effect generated by the lamp. During the reaction, the liquid of the reaction system was collected every 15 min. and the samples were filtered through a Millipore filter prior to the analysis to remove the catalyst particles. The filtrates were analysed by using UV spectrophotometer, Varian, Cary 100. The absorbance of alachlor was monitored at 196 nm and imazaquin at 242 nm respectively. Bromacil, chlorotoluran and sulfosulfuron were monitored at 210, 211 and 214 nm respectively.

3. Results and discussion

3.1. X-ray Diffraction

Samples of TiO_2 immobilised on clay mineral particles were analysed by XRD and are shown in Figure 1. The XRD pattern of anatase is clearly distinct from that of clay mineral particles. The results of XRD give an indication of the extent of TiO_2 crystallisation onto the clay mineral lattice. Two different phases of TiO_2 were observed, in addition to the anatase, a small amount of

127 an additional phase was also observed at 12.8^{o} which are indicated by stars and squares
128 respectively. The average crystallite size calculated using the Scherrer equation is shown in
129 Table 1. Sample (L-Ti (5)100) prepared with the smallest amount of TiO_2 and the lowest
130 hydrothermal temperature, demonstrates the similar reflection peaks of Laponite at 19.5, 34.8,
131 60.8^{o}. In other samples new reflection peaks appeared due to the high dose of anatase
132 crystallisation after the high degree of hydrothermal treatment temperature. These reactions
133 include layer dissolution and crystallisation; as a result the particles of host materials achieve
134 different fabrication through Ti–O–Si bonds (Gun'ko et al., 1998). This crystallisation of TiO_2
135 coincided with an observed loss of opalescence in the corresponding clay mineral structures
136 which presumably results from layer degradation and framework collapse. The crystalline
137 anatase peaks appeared in the samples L-Ti(5)100 and were sharpened in the L-Ti(15)200
138 sample.

139 3.2. N_2 Adsorption

140 The specific surface area of all the Laponite catalysts are in the range of 450-230 m^2/g and were
141 found to decrease upon increasing the anatase content and the hydrothermal temperature (Figure
142 2). It can be further assumed that anatase has a lower surface area than SiO_2. The shape of the N_2
143 adsorption–desorption curves for the samples are quite different depending on the amount of
144 anatase and the hydrothermal temperature, which indicates a different mode of fabrication of the
145 structures in each of the samples. Hysteresis effects were observed in all the samples due the
146 strong interactions of the absorbed gas with the sample surface and results in a delay in
147 desorption (Shaw, 2003). The samples prepared at 150 and 200 ^{o}C show a steep increase in the
148 adsorption from a P/P_0 of about 0.5 which indicates the existence of a very large pore volume of
149 mesopores in the samples (Gregg and Sing, 1982). The large pore volume is mainly from the
150 inter-crystallite voids of anatase nanocrystals and collapsed clay mineral lattice.

151 3.3. FTIR Spectra

152 Figure 3 provides additional evidence for the degree of heterogeneous bonding within the clay
153 mineral particles and there is also evidence that the chemical stability is maintained in the

154 fabrication. Absorption bands of the silica and titania species in the samples are particularly
155 useful for characterising the bonding in the materials. The pure clay mineral sample exhibits a
156 strong adsorption peak at 969 cm^{-1} corresponding to the symmetric vibration of the $(SiO_4)^{4-}$. The
157 adsorption band at around 1087 cm^{-1} displays a shift to a higher frequency as the Si:Ti ratio
158 increases. The shift of Si─O broad stretching band of dehydrated clay mineral particles indicates
159 the formation of bonding between $(SiO_4)^{4-}$ and TiO_2. This band shift is also indicating a small
160 distortion of the symmetry of the tetrahedral sheets. Furthermore, this behaviour can be
161 attributed to an increase in the heterogeneous bonding of Ti─O─Si in the framework, which
162 results in an average decrease in bond strength of Si─O bonds (Hant et al., 2005).

163 3.4. TEM Images

164 Figure 4 present the TEM micrographs of the immobilised TiO_2 on clay mineral particles in
165 different ratios. An interesting feature in the micrographs is the presence of small openings
166 formed by anatase crystals and delamination of mineral layers. Thermal shock and shrinkage in
167 the framework during hydrothermal treatment and subsequent calcination result in the irregular
168 ordering of the porosity. Ordering of Laponite structures has been decreased by an increase in the
169 immobilized TiO_2 which is consistent with the results obtained from XRD experiments.
170 Aggregations of small TiO_2 particles are observed on the clay mineral particles and are
171 increasing with an increase in the amount of TiO_2. Furthermore, most of the anatase particles are
172 poorly crystallised on to the degraded clay mineral network. However, most of the TiO_2 particles
173 are homogenously distributed which help to improve the properties and potential use of these
174 catalysts. TiO_2 nano-particles are partially covering the central holes that facilitate the effective
175 interaction of pollutant molecules with the catalysts.

176 3.5. Raman spectroscopy

177 Figure 5 illustrates the Raman spectra of TiO_2 nanocrystals immobilised on the clay mineral
178 particles. The intensity of the main adsorption peaks at 145, 399, 518 and 640 cm^{-1} increases as
179 the hydrothermal temperature and Ti/clay mineral ratio increases. This result supports the

assumption that anatase TiO_2 nanocrystals were attached to the degraded clay mineral particles. This can be supported with the result obtained from the XRD.

3.6. Photocatalytic activity

In this study we investigate the photocatalytic degradation of a range of herbicides such as bromacil, chlorotoluran, sulfosulfuron, alachlor and imazaquin using immobilised TiO_2 on clay mineral particles. The molecular structures of herbicides are shown in Figure 6. P25 powder was also used to compare the photocatalytic efficiencies of the above mentioned catalysts. This study is to provide an insight into the role of the immobilised anatase crystals on the clay mineral particles as photocatalysts. Figure 7 shows the degradation rate of new catalysts with that of P25. The degradation rates were increased depend on the TiO_2 contents in the fabricated structures. It was found that L-Ti(15)200 and L-Ti(15)150 exhibited significant photocatalytic activity for the degradation of herbicides. It was also observed that the degradation of herbicides in the absence of illumination or without a catalyst were almost negligible. According to these results, it should be noted that the dark adsorption behaviours of all the five catalysts were almost similar and in each case a very low adsorption was observed. The role of adsorption is almost negligible while considering the degradation of herbicides becomes more important. Experimental observations indicated that the 80% of bromacil, chlorotoluran and sulfosulfuron have been removed after UV irradiation for 1 h. Alachlor and imazaquin were removed 60% and 100% respectively after 1 h of UV irradiation. The degradation data was fitted well to a first order rate expression and hence the slop of the lines is proportional to the rate constant. Apparently, the most significant variables for the decomposition of herbicides are the crystallinity of the TiO_2 and the unique pore dimensions. If we compare the photocatalytic activity with respect to the weight percent of the TiO_2 present in fabricated structures, the new catalysts are more active than P25. For instance, during the experiment we used 50 mg of P25 to compare with 50 mg of clay mineral catalyst. In 50 mg catalyst, the amount of titania (anatase phase) is obviously less (mmol of Ti / g of clay) than 50 mg. Therefore the activities per mass of TiO_2 in the new catalysts are superior and the photo-catalytic efficiencies of new catalysts are clearly higher than those of P25. It is also important to understand that the significant differences in the overall performance of the catalysts are likely to be attributed to the physicochemical properties of TiO_2. Earlier studies

show that degradation rate increases with increase in the TiO_2 content (Haque et al., 2006). The crystal size is also an important parameter to ensure the superior activity of a catalyst. The samples with highly crystallised anatase nanocrystals and high porosity not only allow large organic molecules but also light to access the reaction sites. For instance, sample L-Ti(15)200 which has the largest pore volume and crystal size, exhibits the highest photocatalytic activity although samples L-Ti(15)150 and L-Ti(15)100 contain the same dose of titania. It can be noted that the heat treatment transformed titania into structurally stable and rigid crystallites that are attached firmly into clay mineral particles. The temperature of the heat treatment effectively managed to achieve critical particle sizes with photoactive crystallity. The heat treatment involved the shrinkage and collapse of the network onto anatase particles and finally led to the formation of Ti–O–Si bonding. During the shrinkage, the pore volume increases which helps to absorb more pollutants into the active sites of the new catalysts. The specific surface area of the sample is the sum of both the anatase crystals and the clay mineral particles however the photocatalytic activity depends only on the surface area of the anatase crystals. For example, samples L-Ti(15)150 and L-Ti(15)200 (Table 1) have a lower surface area but a high degradation rate than L-Ti(15)100, which has the largest surface area. This observation can be rationalised in terms of crystallinity and the accessible surface area of the anatase nanocrystals, which contributes significantly to the degradation rate.

It should be noted that all the catalysts prepared from Laponite exhibited a higher S_{BET} and pore volume than that of P25. Further observation indicated that the average crystal size of the samples, L-Ti(15)200 and L-Ti(15)150 was almost the same as the crystal size of P25. According to the above facts, there are two factors resulting in the increased photocatalytic activity of L-Ti(15)200 and L-Ti(15)150. The first is the higher pore volume formed by the aggregation of clay mineral particles and second is the TiO_2 contents. Furthermore, the TiO_2 contents attached to the clay mineral particles have an optimal crystal size to enhance the photocatalytic reactions. During the degradation process, herbicides and its intermediates may be penetrated into the interlayer surface and make close vicinity to TiO_2, thus allow these compounds to be easily accessible to the photocatalytic sites of anatase and are finally decomposed completely. Moreover, the newly prepared catalysts show another important

practical benefit due to its easy recovery from the water dispersions by filtration. The milky suspensions of P25 takes several hours to sediment compared to new solid porous catalysts.

4. Conclusions

The photocatalytic degradation of bromacil, chlorotoluran, sulfosulfuron, alachlor and imazaquin were studied with a new structure of anatase crystals linked to Laponite particles. The catalysts synthesised at 200 and 150 ^{o}C with 15 mmol of Ti / g of clay mineral ratios showed better photoactivity. This can be attributed to the fact that the new catalysts maintained a critical crystallite size and a higher pore volume. A mesoporous structure of clay mineral particles opens pathways to the interior of the crystals, through which pollutants could be transported to interact with the anatase surface. If the photoactivity is compared in terms of unit mass of TiO_2 present in the new clay catalysts then P25 is technically less active. The amount of photoactive phase in the new clay catalyst is much less than P25, however the activity is much higher than P25 when the activity is considered by per mass of TiO_2. The sedimentation rates of new catalysts are much better compared to P25 and can easily be filtered out from the dispersions. **Acknowledgments**

This work was supported by Australian Research Council (ARC). The author is gratefully acknowledged Prof. H.Y. Zhu for his aid in the data analysis.

References

Beydoun, D., R. Amal, G.K.C. Low and S. McEvoy, 2000. Novel photocatalyst: Titania-coated magnetite. Activity and photodissolution. J. Phy. Chem. B, 104(18): 4387-4396.

Chen, H., A. Matsumoto, N. Nishimiya and K. Tsutsumi, 1999. Preparation and characterization of TiO_2 incorporated y-zeolite. Colloids Surf. A, 157(1-3): 295-305.

Chu, W. and C.C. Wong, 2004. Study of herbicide alachlor removal in a photocatalytic process through the examination of the reaction mechanism. Ind. Eng. Chem. Res., 43(17): 5027-5031.

Garcia, J.C. and K. Takashima, 2003. Photocatalytic degradation of imazaquin in an aqueous suspension of titanium dioxide. J. Photochem. Photobiol. A 155(1-3): 215-222.

Gregg, S.J. and K.S.W. Sing, 1982. Adsorption, surface area and porosity. 2nd ed. Edn., New York: Academic press.

Gun'ko, V.M., V.I. Zarko, V.V. Turov, R. Leboda, E. Chibowski, L. Holysz, E.M. Pakhlov, E.F. Voronin, V.V. Dudnik and Y.I. Gornikov, 1998. CVD-titania on fumed silica substrate. J. Colloid Interface Sci.198(1): 141-156.

Hant, S.M., G.S. Attard, R. Riddle and K.M. Ryan, 2005. Periodic binary Si:Ti, Si:Al mixed macroporous oxides with ultrahigh heteroatom loading: A facile sol-gel approach. Chem. Mater., 17(6): 1434-1440.

Haque, M.M., M. Muneer and D.W. Bahnemann, 2006. Semiconductor-mediated photocatalyzed degradation of a herbicide derivative, chlorotoluron, in aqueous suspensions. Environ. Sci.Technol., 40(15): 4765-4770.

Kim, M.S., C.S. Ryu and B.W. Kim, 2005. Effect of ferric ion added on photodegradation of alachlor in the presence of TiO_2 and UV radiation. Water Res., 39(4): 525-532.

Kuwahara, Y., T. Kamegawa, K. Mori and H. Yamashita, 2008. Fabrication of hydrophobic zeolites using triethoxyfluorosilane and their application as supports for TiO_2 photocatalysts. Chem. Commun.(39): 4783-4785.

Liu, X.S., K.K. Iu and J.K. Thomas, 1992. Encapsulation of TiO_2 in zeolite y. Chem. Phys. Lett., 195(2-3): 163-168.

Long, R.Q. and R.T. Yang, 2000. Characterization of Fe-ZSM-5 catalyst for selective catalytic reduction of nitric oxide by ammonia. J. Catal., 194(1): 80-90.

Mori, K., Y. Kondo, S. Morimoto and H. Yamashita, 2007. Multifunctional heterogeneous catalyst: Titanium-containing mesoporous silica material encapsulating magnetic iron oxide nanoparticles. Chem. Lett., 36(8): 1068-1069.

Palmisano, G., V. Augugliaro, M. Pagliaro and L. Palmisano, 2007. Photocatalysis: A promising route for 21st century organic chemistry. Chem. Commu.(33): 3425-3437.

Prieto-Mahaney, O.O., N. Murakami, R. Abe and B. Ohtani, 2009. Correlation between photocatalytic activities and structural and physical properties of titanium(iv) oxide powders. Chem. Lett., 38(3): 238-239.

Rodionova, G.P., A.A. Perminov and N.S. Smirnov, 1978. A comparative study of natural clays and the synthetic Laponite. 35(12): 743-745.

Rodriguez, P., V. Meille, S. Pallier and M.A. Al Sawah, 2009. Deposition and characterisation of TiO_2 coatings on various supports for structured photocatalytic reactors. Appl. Catal. A-Gen., 360(2): 154-162.

Ryu, C.S., M.S. Kim and B.W. Kim, 2003. Photodegradation of alachlor with the TiO_2 film immobilised on the glass tube in aqueous solution. Chemosphere, 53(7): 765-771.

Shaw, D., 2003. Introduction to colloid and surface chemistry. Elsevier, New York.

Sterte, J., 1986. Synthesis and properties of titanium oxide cross-linked montmorillonite. Clays Clay Miner. 34(6): 658-664.

Takeda, N., M. Ohtani, T. Torimoto, S. Kuwabata and H. Yoneyama, 1997. Evaluation of diffusibility of adsorbed propionaldehyde on titanium dioxide-loaded adsorbent photocatalyst films from its photodecomposition rate. J. Phys. Chem. B, 101(14): 2644-2649.

Wong, C.C. and W. Chu, 2003. The direct photolysis and photocatalytic degradation of alachlor at different TiO_2 and UV sources. Chemosphere, 50(8): 981-987.

Wong, C.C. and W. Chu, 2003. The hydrogen peroxide-assisted photocatalytic degradation of alachlor in TiO_2 suspensions. Environ. Sci. Technol., 37(10): 2310-2316.

Yamashita, H. and M. Anpo, 2003. Local structures and photocatalytic reactivities of the titanium oxide and chromium oxide species incorporated within micro and mesoporous zeolite materials: XAFS and photoluminescence studies. Curr. Opin. Solid State Mater. Sci., 7(6): 471-481.

Yamashita, H. and K. Mori, 2007. Applications of single-site photocatalysts implanted within the silica matrixes of zeolite and mesoporous silica. Chem. Lett., 36(3): 348-353.

Yamashita, H., K. Yoshizawa, M. Ariyuki, S. Higashimoto, M. Che and M. Anpo, 2001. Photocatalytic reactions on chromium containing mesoporous silica molecular sieves (Cr-HMS) under visible light irradiation: Decomposition of no and partial oxidation of propane. Chem. Commun.(5): 435-436.

Yang, R.T. and W.B. Li, 1995. Ion-exchange pillared clays- a new class of catalysts for selective catalytic reduction of no by hydrocarbons and by ammonia. J. Catal., 155(2): 414-417.

Yang, X.Z., Y. Dongjiang, H.Y. Zhu, J.W. Liu, W.N. Martins, R. Frost, L. Daniel and Y.N. Shen, 2009. Mesoporous structure with size controllable anatase attached on silicate layers for efficient photocatalysis. J. Phys. Chem. C, 113(19): 8243-8248.

Zhu, H.Y., J.A. Orthman, J.Y. Li, J.C. Zhao, G.J. Churchman and E.F. Vansant, 2002. Novel composites of TiO_2 (anatase) and silicate nanoparticles. Chem. Mater., 14(12): 5037-5044.

FIGURES

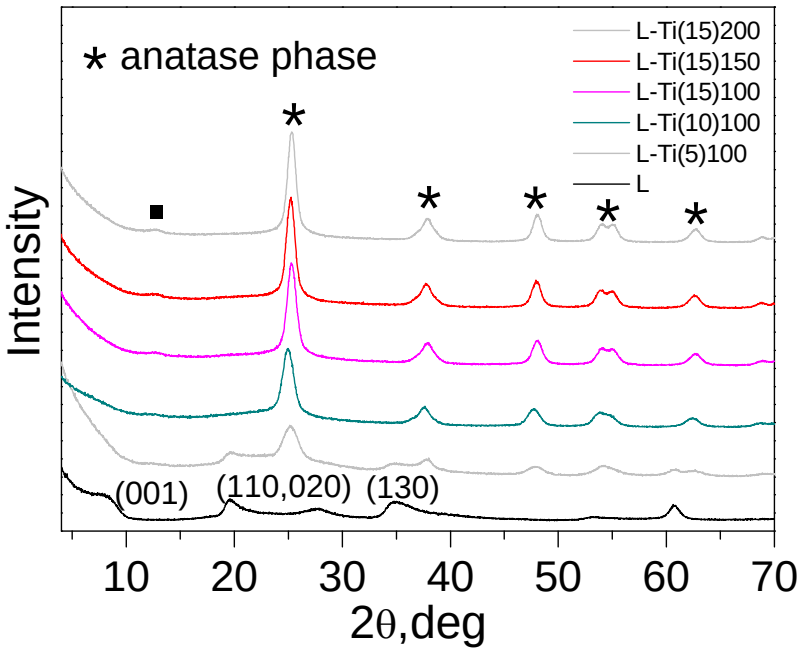

Fig. 1

337

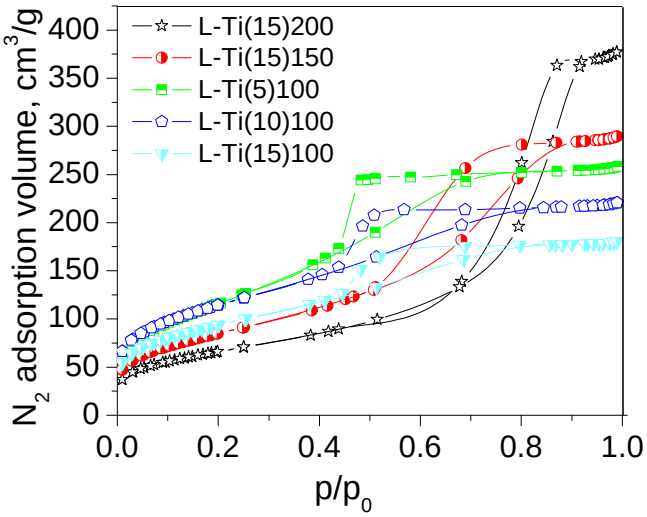

338

339 **Fig. 2**

340

341

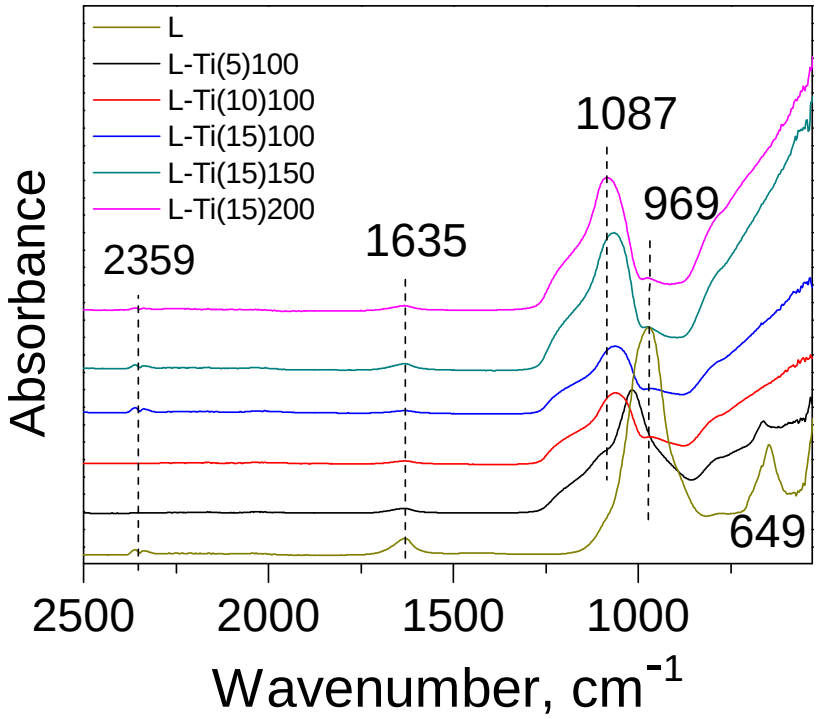

342

343 **Fig. 3**

344

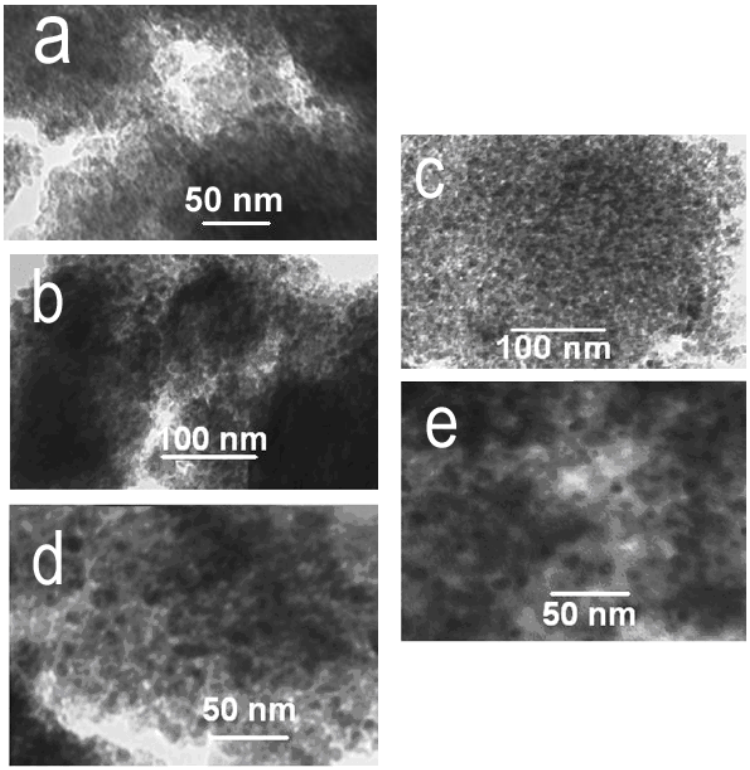

345

346 **Fig. 4**

347

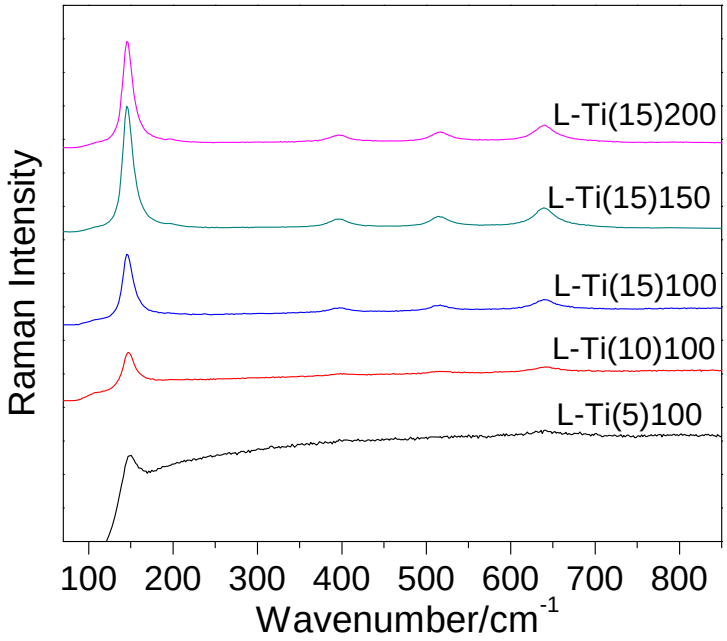

348

349 **Fig. 5**

350

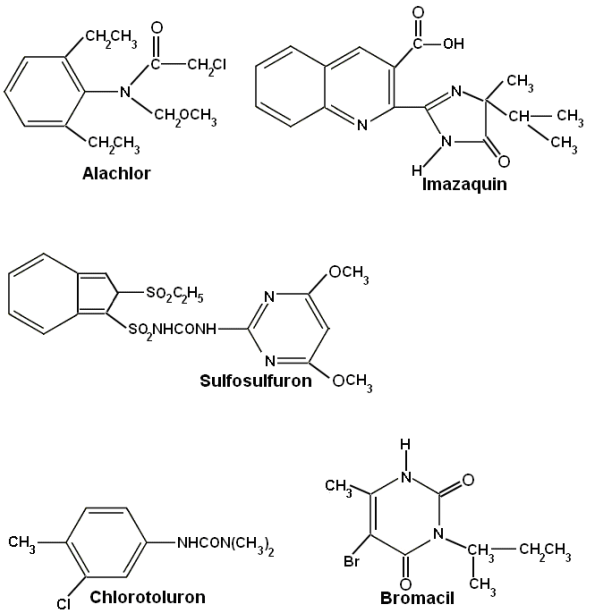

351

352 **Fig. 6**

353

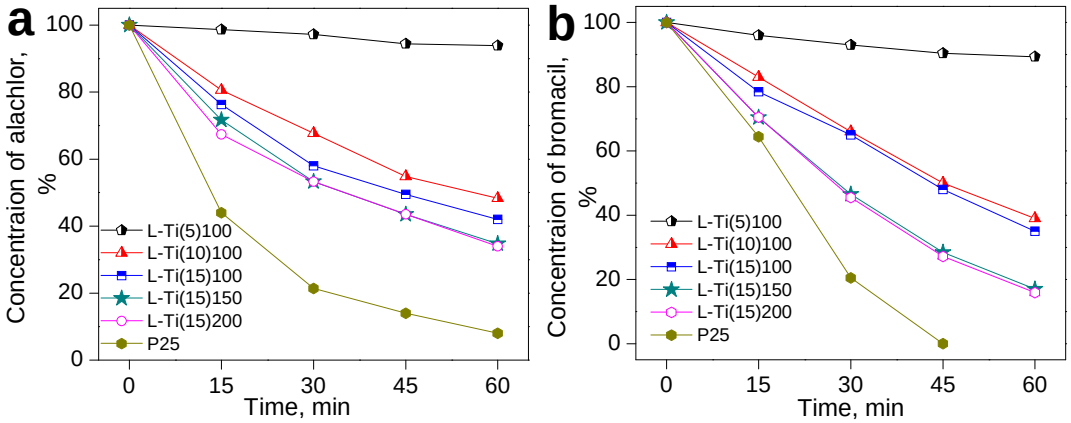

354

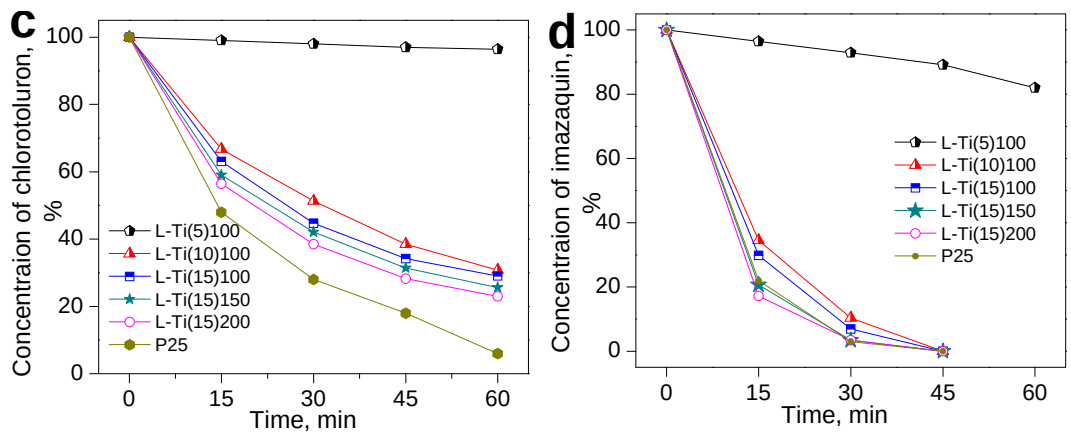

355

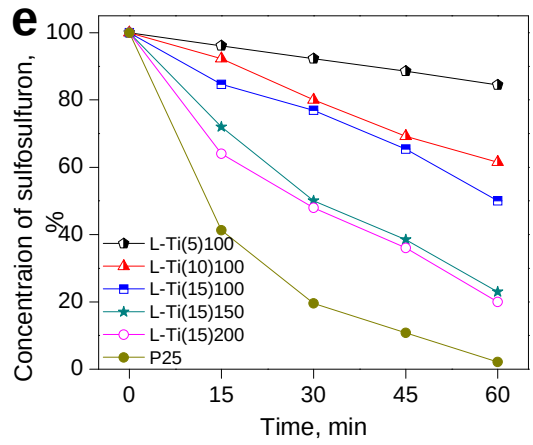

356

357 **Fig. 7**

358

List of Figures

List of Tables

Table 1. Specific surface area, porous volume and mean anatase crystal size.

Samples	$S_{BET}(m^2.g^{-1})$	V_p[a]$(cm^3.g^{-1})$	D_A (nm)
L-Ti(5)100	420	0.38	4.3
L-Ti(10)100	398	0.31	5.9
L-Ti(15)100	340	0.29	7.6
L-Ti(15)150	315	0.43	7.7
L-Ti(15)200	232	0.55	8.5
P25	49.9	0.092	8.3

[a] Single point adsorption total pore volume of pores at P/P_0 0.99, Mean anatase crystal size (D_A) was calculated by using the Scherrer equation.